

DOI: 10.1002/adfm.200700296

# Growth of Magnetic Yard-Glass Shaped Boron Nitride Nanotubes with Periodic Iron Nanoparticles\*\*

By Zhi-Gang Chen, Jin Zou, Feng Li, Gang Liu, Dai-Ming Tang, Da Li, Chang Liu, Xiuliang Ma, Hui-Ming Cheng,\* Gao Qing Lu,\* and Zhidong Zhang

Novel yard-glass shaped boron nitride nanotubes (YG-BNNTs) periodically filled with Fe nanoparticles were synthesized by a catalytic reaction process of ammonia with boron precursors at 1300 °C. Such novel structures were extensively characterized using X-ray diffraction and advanced electron microscopy. The Fe-filled boron nitride nanotubes show excellent ferromagnetic properties at room temperature with superior chemical stability. A growth model is proposed for the formation of such novel BN nanostructures.

## 1. Introduction

Confinement of nanosized metal and compounds in nanotubes often lead to nanoscale hybrid systems with unique optical, electronic and/or magnetic properties.<sup>[1]</sup> Thus, encapsulation of foreign materials inside nanotubes has the potential to widen the routes to engineer novel nanoscale devices with unique performances.<sup>[2]</sup> For example, production of magnetic hybrid systems by filling nanotubes with magnetic particles can be used as magnetic data storage, magnetic toners, magnetic inks, ferrofluids, and contrast agents for magnetic resonance imaging,<sup>[2,3a]</sup> and functionalized boron nitride nanotubes (BNNTs) with oxides or biomolecules can be used for sensor and nano/bio- applications.<sup>[3b,c]</sup> So far, various metals, carbides, nitrides, oxides, and fullerenes have been encapsulated in nanotubes.<sup>[4]</sup> However, it is a great challenge to periodically encapsulate nanoparticles (particular magnetic nanoparticles) within nanotube building blocks in situ, and to align the nanoparticles in one dimensional nanostructures.

Hexagonal BNNTs have unique physical properties, such as uniform semiconducting behavior with a wide bandgap of ~5.5 eV, which, unlike carbon nanotubes (CNTs), depend weakly upon the chirality and lateral size.<sup>[5]</sup> Moreover, BNNTs are chemically inert and thermally stable than CNTs.<sup>[6]</sup> Therefore, a BNNT may serve as a naturally insulating and/or protective shield for encapsulated foreign materials.<sup>[7]</sup> Of great significance, magnetic nanoparticles periodically filling within high temperature inert nanotube building blocks may give rise to novel physical phenomena in high temperature magnetism and nano-electromagnetism. To date, since the first observation of Bamboo-shaped BNNTs,<sup>[8]</sup> different morphologies of BNNTs and corresponding growth mechanisms have been reported.<sup>[9–12]</sup> However, metal nanoparticles periodically filled nanotubes have been rarely reported.<sup>[10–12]</sup>

In this study, we demonstrate a simple method to synthesize yard-glass (YG) shaped BNNTs periodically filled with magnetic Fe nanoparticles using a floating catalyst method and such synthesized YG-BNNTs possess unique magnetic properties. Based on structural characterization, the formation mechanism is studied by a proposed model and discussed.

## 2. Results and Discussions

### 2.1. Characterization

In a typical synthesis, precursors of B-N-O-Fe powders were heated to 1300 °C for 2 h in a mixed gas of NH<sub>3</sub> and Ar to fabricate YG-BNNTs, (for details see Experimental). Figure 1a is a typical low magnification scanning electron microscopy (SEM) image and shows a high density of one dimensional (1D) nanostructures with their diameters being in the range of 50–800 nm and the length of tens to hundreds of micrometers. By careful examination of their morphology, one can recognize that, for any single 1D nanostructure, knob-like nodes are periodically appeared. To understand their detailed morphology, high magnification SEM observation was carried out. Fig-

[\*] Prof. H.-M. Cheng, Z.-G. Chen, Dr. F. Li, G. Liu, D.-M. Tang, D. Li, Prof. C. Liu, Prof. X. Ma, Prof. Z. Zhang  
Shenyang National Laboratory for Materials Science  
Institute of Metal Research, Chinese Academy of Sciences  
Shenyang (P.R. China)  
E-mail: cheng@imr.ac.cn

Prof. G. Q. (Max) Lu, Z.-G. Chen  
ARC Centre for Functional Nanomaterials  
The University of Queensland  
Brisbane (Australia)  
E-mail: maxlu@uq.edu.au

Dr. J. Zou  
School of Engineering and Centre for Microscopy and Microanalysis  
The University of Queensland  
Brisbane (Australia)

[\*\*] We would like to thank Mr. Kuiyi Hu, Bo Wu, and Hua Guo for their assistance. This work was supported by the Key Research Program of MOST, China (2006CB932703) and Australian Research Council through its Centres of Excellence Scheme.

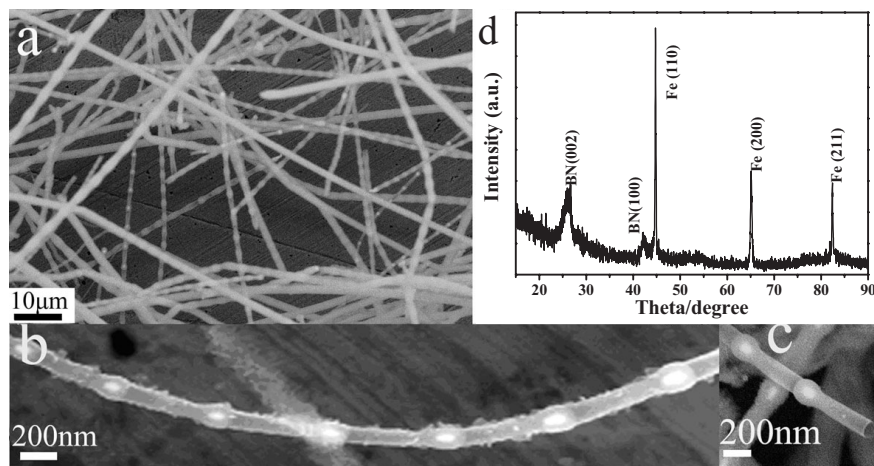


**Figure 1.** SEM images of YG-BNNTs. a) A typical low-magnification image. b,c) Typical high-magnification images showing uniform units connection and an open end of the tube, respectively. d) XRD patterns showing two crystalline phases—hexagonal BN and  $\alpha$ -Fe.

ure 1b and c show their detailed morphological characteristics: (1) these 1D nanostructures have a tube-like morphology, (2) each tube is formed by a number of uniform (in shape and size) YG units, (3) each YG unit has an open end and a closed end, and (4) catalyst nanoparticles were periodically filled at the closed ends but no catalyst nanoparticles found at the open ends. Figure 1d is a XRD pattern of YG formed tubes, showing clearly that they are composed of only two crystalline phases: hexagonal BN structure with  $a = 0.2504$  nm and  $b = 0.6656$  nm (JCPDS 34-0421) and  $\alpha$ -Fe structure with  $a = 0.2866$  nm (JCPDS 06-0696). This suggests that the catalyst nanoparticles filled inside the tubes might be  $\alpha$ -Fe metal nanoparticles and the tubes might be made of hexagonal BN, i.e., the synthesized nanostructures are YG-BNNTs, with periodically filled Fe nanoparticles. Extensive SEM investigations suggest that the purity of YG-BNNTs in the final product was over 90%, the impurities of products are Fe nanoparticles coated with BN.

To further understand the microstructure of YG-BNNTs, transmission electron microscopy (TEM) characterization was conducted. Figure 2 shows several typical bright-field TEM images, revealing different morphologies of YG-BNNTs. Figure 2a is a low magnification TEM image, showing that the catalyst nanoparticles are filled in all closed ends of yard-glass units, regardless the lateral size of tubes. As can be seen from Figure 2a, for a given tube, all yard-glass units and their filled catalyst nanoparticles are uniform in shape and size. Furthermore, it is observed that smaller tubes are encapsulated in larger ones as evidenced in Figure 2a (marked by arrows). In this case, a smaller tube is fully enclosed in a large yard-glass unit, as shown in the inset of Figure 2a. Whilst in Figure 2b, a relatively straight smaller tube is filled into a large yard-glass unit from its open end.

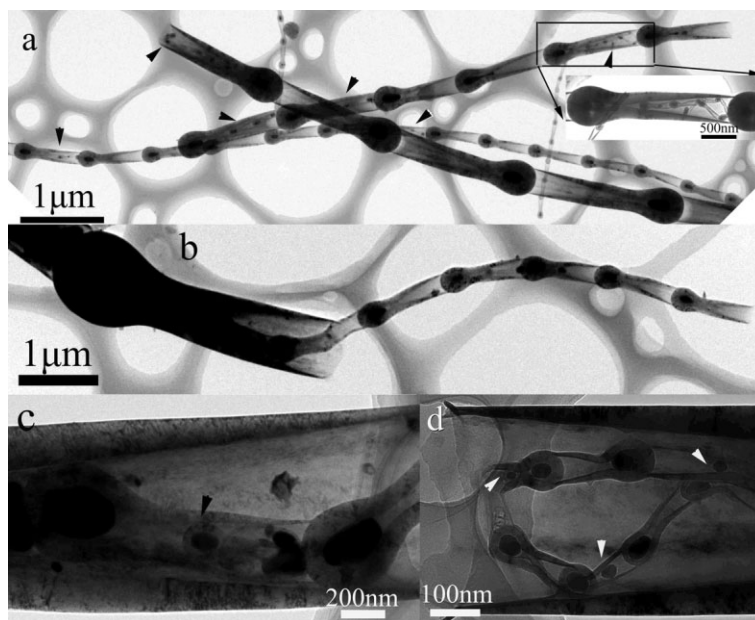


**Figure 2.** TEM images of YG tubes. a) Catalyst nanoparticles filled in all YG units and smaller tubes are observed inside larger ones (marked by arrows). Inset: a typical inside tube; b) Image revealing a straight small tube filling inside a large yard-glass unit from its open end. c) Russian-Matryoshka structured tube. d) Nanoparticles inside YG units—marked by arrows.

Occasionally, Russian-Matryoshka structured tubes can also be observed, as shown in Figure 2c, and nanoparticles can be found in the middle of YG units without touching the open/close ends (marked by arrows in Fig. 2d). Extensive TEM examination of these YG-BNNTs shows that (1) almost all the tubes have the periodical Fe filled morphology, (2) at least over 10% of yard-glass units are filled by smaller tubes and (3) no catalysts have been found at the open ends of YG BNNTs, which are consistent with SEM characterization.

To determine their chemical composition, the synthesized YG tubes were studied using energy filtered TEM,<sup>[13]</sup> which gives images mapping B, N, C, separately. Images were formed with the energy loss windows centered respectively at the B K edge of 188 eV, the N K edge of 401 eV, and the C K edge of 284 eV, and with slit sizes of 10 eV, 20 eV and 16 eV, respectively. Examples are shown in Figure 3a–d. Figure 3a is an image using electrons with zero energy loss, showing two connecting YG units on the holey C film. Figure 3b and c are B and N maps, which clearly show the presence of B and N. Figure 3d is a C map, in which the holey C film is clearly shown. However, the disappearance of C signal in the YG units and the decreased intensity in the overlapping region between YG units and C film (due to the multiple scattering ef-

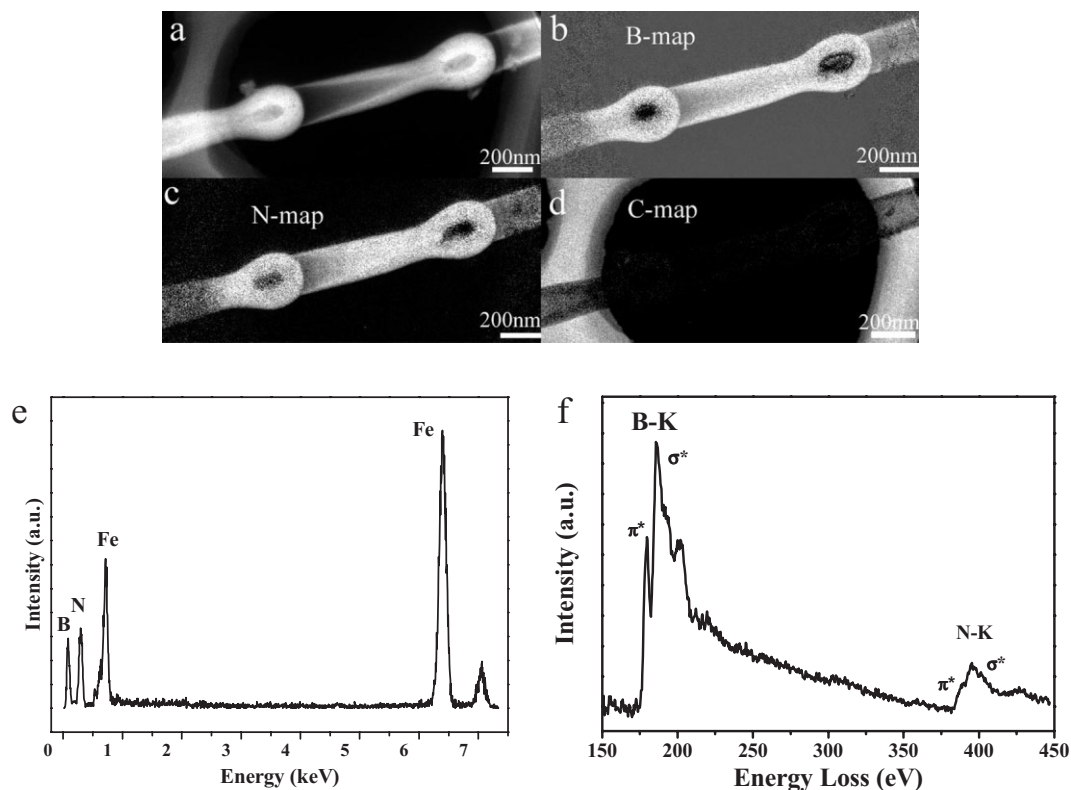


**Figure 3.** a) A zero-loss image of the two YG units. b–d) Elemental maps (B, N and C) implying the uniform distribution of B and N within YG unit. e) EDS analysis of the knob. f) EELS analysis of tubes.

fects) in Figure 4d suggest that the synthesized YG tubes are BN only. Since energy filtered TEM requires very thin TEM specimens (to avoid multiple scattering), it is not possible to perform energy filtered TEM on the catalyst particles as their size (~100 nm) is far beyond the required single scattering criteria. Nevertheless, the chemical compositions of catalyst particles can be determined by the energy dispersive spectroscopy (EDS). Figure 3e is a typical EDS taken from the knob region, which shows the characteristic ionization edges of B, N, and Fe. This confirms that the catalyst nanoparticles are Fe, which matches well with the XRD result. No O and C were found in the EDS profile. Furthermore, quasi-quantitative analysis gives the ratio of B/N is close to 1. To further confirm the structure of BN tubes and the absence of C in the synthesized tubes, electron energy loss spectroscopy (EELS) was used to study several tens of tubes. Figure 3f is a typical EELS profile and shows sharp  $\pi^*$ -peaks on the left side of both B and N K edges, indicating that the tubes has the  $sp^2$ -bonding, i.e., the hexagonal structure. Quantitative analysis of EELS spectrums gives a B/N atomic ratio of  $1.0 \pm 0.1$ . No carbon was detected in the EELS profile, suggesting again that the tubes are pure BN which is consistent with energy filtering TEM results. All these TEM results are in consistent with the XRD result, hexagonal BN and  $\alpha$ -Fe.

To dissect how these YG units connect and form YG-BNNTs, high-resolution (HR) TEM was performed. Figure 4a shows a typical microstructure of a joint between two YG units.

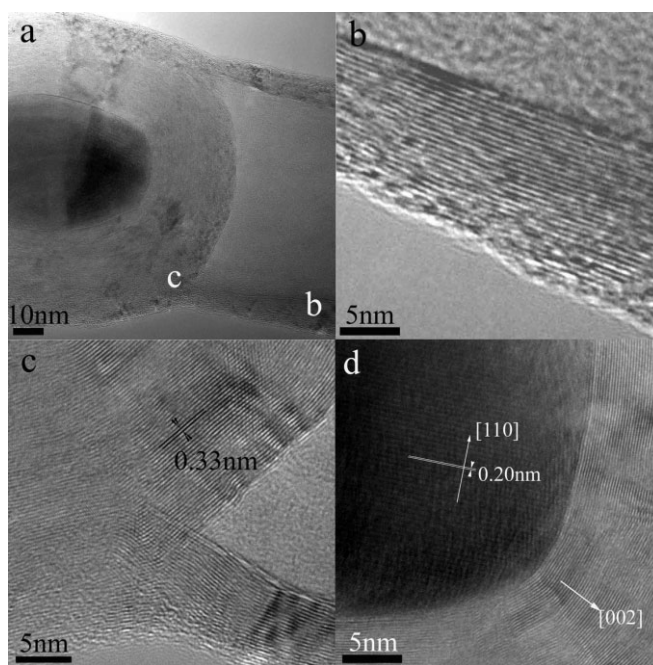


**Figure 4.** TEM images showing well crystallized BN and faceted Fe nanoparticles. a) joint of two adjacent yard-glass units, in which a faceted Fe nanoparticle can be clearly seen. b) A segment of yard-glass unit near the open end showing well crystallized BN layered structure. c) Details of the joint showing well crystallized BN layered structure in the closed ends and the joint. d) The Fe nanoparticles showing crystallized nature and connection with the BN shell.

HR-TEM observations from different locations (as marked in Fig. 4a) are given in Figure 4b–d. Figure 4b clearly displays that the wall thickness decreases gradually with the BN layers at the outer surface gradually disappearing towards the open end and those at the inner surface extending to the open ends. Figure 4c reveals the detailed joint structure, in which a thin wall inserts into the large knob, which is tightly connected. Both the wall and knob are well-crystallized with the identical lattice spacing of  $\sim 0.33$  nm (corresponding to the  $d_{0002}$  spacing in bulk hexagonal BN). Figure 4d shows that the nanoparticle has different facets covered with curved BN layers and that the lattice fringe of the nanoparticle is about 0.20 nm, corresponding to the {110} crystal planes of  $\alpha$ -Fe.

## 2.2. Magnetic Properties

The magnetic hysteresis loops of the YG-BNNTs were measured between a magnetic field of  $\pm 50$  kOe at 300 K using a superconducting quantum interference device (SQUID) magnetometer, as shown in Figure 5a and b. For BCC  $\alpha$ -Fe, the critical size for single domain particles exhibiting the superparamagnetic property is  $\sim 20$  nm; above which, there will be domain walls in the particles that show the ferromagnetic property.<sup>[14]</sup> The size of Fe catalyst particles in this study is mainly distributed from  $\sim 20$  nm to 500 nm through a statistical analysis (shown in Fig. 5c) of a large number of TEM images. As a consequence, Fe particles in our products should exhibit ferromagnetic property. From Figure 5a, it is evident that the as-prepared YG-BNNTs exhibit the typical ferromagnetic behavior. The value of the saturation magnetization  $M_s$  of the as-prepared YG-BNNTs is  $162 \text{ emu g}^{-1}$ , which is lower than that of

bulk Fe ( $M_s = 222 \text{ emu g}^{-1}$ ) due to the weight fraction of a very small amount of Fe nanoparticles with superparamagnetism and the BN shells.<sup>[15]</sup> From the enlarged section of the hysteresis loop for the as-prepared sample (Fig. 5b), one can clearly see that the values of remnant magnetization  $M_r$  and coercivity are  $0.33 \text{ emu g}^{-1}$  and  $\sim 9.5$  Oe, respectively. Compared to the coercivity of bulk Fe ( $H_c \sim 0.9$  Oe), the coercivity of the encapsulated Fe particles in the YG-BNNTs is ten times stronger. It is worth to mention that the hysteresis loop of the YG-BNNTs exposed in the air for 30 days is almost overlapped with that of the as-prepared YG-BNNTs (Fig. 5a). It means that the magnetic properties of the Fe nanoparticles encapsulated in the YG-BNNTs are well preserved, although the YG-BNNTs have been exposed to the air for a long time. That is, the Fe nanoparticles encapsulated by the BN shells can be well protected from the oxidation by the atmosphere, so that this kind of YG-BNNTs may be used in rigorous environments for nano-scaled magnetic devices.<sup>[16]</sup>

## 2.3. Growth Mechanism

It is of interest to note that, as mentioned earlier, over 10% YG units have smaller tubes filled inside them. In addition, Russian-Matryoshka structured YG-BNNTs (Fig. 2c) can be also found. These novel structures cannot be possibly explained by the conventional sequential growth model,<sup>[9c,10,11,12c,d]</sup> in which catalysts are often found at the open ends (tips of tubes). Therefore, there must be an alternative growth model. Furthermore, for the tubes formed in the conventional sequential growth model, the nanoparticles are not necessarily uniform in size if there is any inside the tubes,<sup>[11]</sup> but it is necessary for

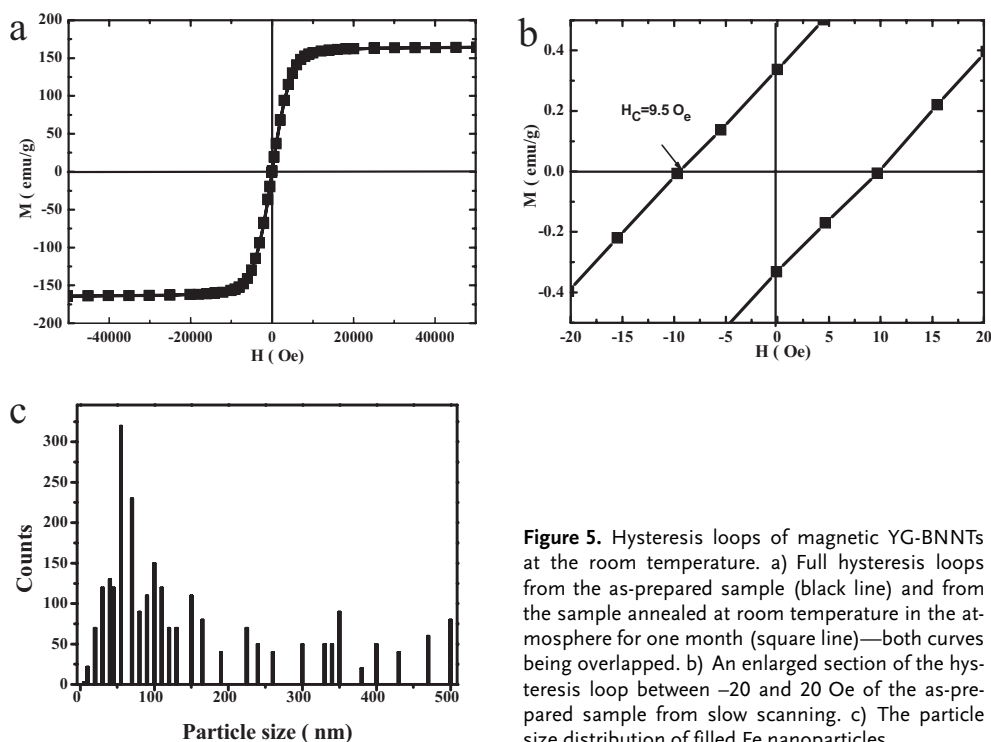


**Figure 5.** Hysteresis loops of magnetic YG-BNNTs at the room temperature. a) Full hysteresis loops from the as-prepared sample (black line) and from the sample annealed at room temperature in the atmosphere for one month (square line)—both curves being overlapped. b) An enlarged section of the hysteresis loop between  $-20$  and  $20$  Oe of the as-prepared sample from slow scanning. c) The particle size distribution of filled Fe nanoparticles.

these nanoparticles to be located at the knobs if they appear.<sup>[9c,11]</sup> However, in our case, for a given tube, the size of nanoparticles is identical and individual nanoparticles can be occasionally found in the middle of YG units (refer to Fig. 2d). In addition, no nanoparticle can be found at the tips of YG-BNNTs. As far as all these evidences are concerned, we can conclude that the formation of synthesized YG-BNNTs is not governed by the conventional sequential growth model.

To elucidate the possible formation mechanism, intermediate microstructures of YG-BNNTs were studied by significantly reducing the reaction time (5 min). It has been found that the majority of YG-BNNTs are short, generally consisting of up to 4 YG units for each tube. Figure 6 shows their typical structures. It is of interest to note that (1) single YG units can be clearly identified (Fig. 6a) albeit with a very small number in the sample, indicating that single YG unit would not like to

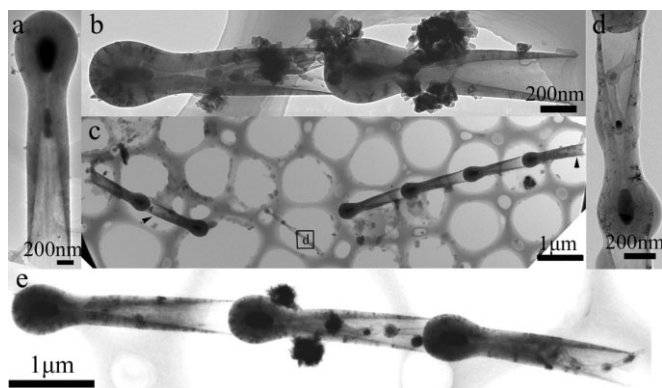


**Figure 6.** TEM of quenched samples. a) Single yard-glass unit. b) Two units with small tubes filling in large ones. c) Tubes consisting of up to 4 yard-glass units. d) Enlarge image of the area marked with d in (c). e) One small tube filling inside a large yard-glass unit from its open end and other filling inside a unit.

stay as their own; (2) almost all large tubes are filled with smaller tubes with similar or less numbers of YG units (refer to Fig. 6b–d); (3) small tubes are occasionally found to be filled into the open ends of larger tubes with identical alignment with the larger ones, which further substantiating that the conventional catalyst sequential growth model can not be used in our case (refer to Fig. 6e). These experimental facts lead us to believe that the catalyst filled YG units should be formed first. As for one tube, since these YG units are formed in gaseous phase, it is reasonable to expect some YG units to have the identical morphology. A single YG-BNNT can then be formed by joining these identical YG units together.

The question now is what is the driving force for aligning and connecting these YG units together. To answer this question, we note that the gas flows, particularly at the elevated temperature, could assist nanostructure alignment. In addition, the magnetic nature of Fe-filled BNNTs can promote such units to be aligned. Furthermore, the system tends to minimize the total energy of the tubes by connecting individual unit together due to the total energy minimization (predominantly surface

energy). Therefore, we believe that the synthesized YG-BNNTs were formed by the connection of sequentially aligned YG units with similar sizes. Our extensive characterization results suggest the following scenario for the formation of YG-BNNTs, as schematically illustrated in Figure 7.

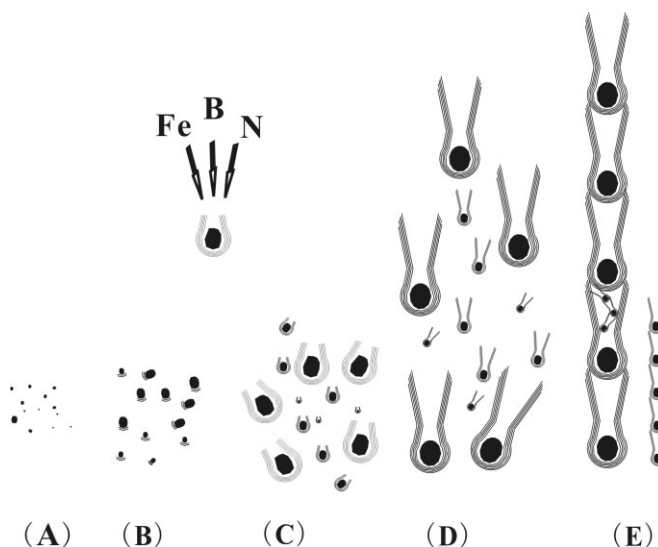


**Figure 7.** The catalytic layered epitaxial assembly and simultaneous axial connection model growth model for YG-BNNTs.

(A) Large quantity of Fe nanoparticles is formed by ferrocene decomposition, floating around at the elevated temperature and in quasi-liquid form.<sup>[9c,10,11]</sup>

(B) These Fe nanoparticles serve as catalysts. Transitional products (BO) reacting with ammonia on the surface of these catalyst nanoparticles will produce N and B atoms, which then diffuse on the surface of Fe catalyst nanoparticles to form BN species. When the BN species are supersaturated, it begins to precipitate layer by layer in the form of BN sheets around the surface of Fe catalyst nanoparticles.

(C) With inward growth of BN layer at the interface between the earlier formed BN and the faceted Fe, the increased curvature of the newly formed BN layer increases the strain energy of BN layers.<sup>[9c,10,11]</sup> Simultaneously, BN shell is growing faster than the Fe nanoparticle, leading to higher strain energy. BN shells gradually cover the whole hemi-sphere of the Fe particle, while the Fe catalyst continues to precipitate the supersaturated BN species epitaxially over the surface of Fe particles, leading to YG shaped units.

(D-E) The YG units readily float in gas at the elevated temperature and are aligned (possibly assisted by their magnetic nature due to presence of Fe nanoparticles), those units with similar size then join together to form tubes due to the gas buoyancy and the total energy minimization (surface energy and strain energy). During this process, smaller tubes and metal catalysts also have the opportunity to be filled into the larger YG units. In the special cases, the Russian-Matryoshka structured tubes can be formed. This growth model could be de-

scribed as the catalytic layered epitaxial assembly and simultaneous axial connection model, which is very different to the classic root growth model in which an entire tube is grown from catalyst nanoparticles at the tip,<sup>[4d,9c,10,11]</sup> whereas, in our case, the tubes are formed through the connection of identical units.

### 3. Conclusions

Novel YG-BNNTs were synthesized by a floating catalytic process of ammonia reacting with boron precursors. Excellent ferromagnetic property of the YG-BNNTs was observed up to room temperature, indicating that these novel magnetic YG-BNNTs have significant application potentials in fabricating nano-scaled electromagnetic devices. The formation of synthesized YG-BNNTs cannot be explained by the conventional model. A growth model for these novel YG-BNNTs is proposed based on the experimental results.

### 4. Experimental

Periodically Fe-filled YG-BNNTs were grown by catalytic decomposition of ammonia at a temperature of 1300 °C using a floating catalyst method. The temperature of the central region of the multi-zone furnace was increased at a rate of 35 °C min<sup>-1</sup> to 1300 °C and maintained at that temperature for 120 min. High purity streams of Ar (at a rate of 50 sccm) and NH<sub>3</sub> (at a rate of 175 sccm) were used as the carrier and reaction gases, respectively. The raw materials, ball milled mixture of B-O-Fe precursors (about 0.7 g, B:B<sub>2</sub>O<sub>3</sub>:Fe<sub>2</sub>O<sub>3</sub> = 1:7:2, mass ratio) for 3 h under the ammonia to form B-N-O-Fe precursors, were loaded into a BN crucible at the center of an Al<sub>2</sub>O<sub>3</sub> tube (diameter of 32 cm, length of 100 cm) which was located in the horizontal tube furnace. The catalysts (ferrocene about 0.1 g) are placed at the front end of the furnace, where the temperature was maintained at 200 °C. After the furnace was cooled to room temperature, white filament-like products were collected around the thermal couple above the crucible.

The formation process involves the floating catalyst catalyzed decomposition ammonia, in which the main reactions would be:



Ferrocene is a critical reagent for the formation of periodically iron-filled YG tubes. During the process, ferrocene vaporizes slowly and flows to the reaction zone and decomposes quickly into iron and containing-carbon gas. The resultant iron catalyst would be in the form of semi-liquid nanoparticles floating in gas at the elevated temperature (1300 °C). In the crucible, amorphous B powders react with B<sub>2</sub>O<sub>3</sub> to form the intermediate products (BO) with the help of Fe<sub>2</sub>O<sub>3</sub> catalysts. The intermediate products (BO) are easy to vaporize. With the presence of the Fe nanoparticles as catalysts, the transition products react with ammonia to form novel yard-glass BN nanotubes.

The products were characterized using XRD (XRD, RINT2200, Cu K $\alpha$ ), SEM (Leo Super35), and TEM (Tecnai F30 equipped with EELS and EDS). The magnetic property of YG-BNNTs was measured using a SQUID magnetometer (Quantum Design).

Received: March 12, 2007

Revised: May 1, 2007

Published online: October 4, 2007

- [1] Y. H. Gao, Y. Bando, *Nature* **2002**, *415*, 599.
- [2] a) P. M. Ajayan, S. Iijima, *Nature* **1993**, *361*, 333. b) C. Guerret-Piecourt, Y. Lebourar, A. Loiseau, H. Pascard, *Nature* **1994**, *372*, 761. c) H. Dai, E. W. Wong, Y. Z. Lu, S. Fan, C. M. Lieber, *Nature* **1995**, *375*, 769.
- [3] a) G. Korneva, H. H. Ye, Y. Gogotsi, D. Halverson, G. Friedman, J. C. Bradley, K. G. Kornev, *Nano Lett.* **2005**, *5*, 879. b) W.-Q. Han, A. Zettl, *J. Am. Chem. Soc.* **2003**, *125*, 2062. c) C. Y. Zhi, Y. Bando, C. C. Tang, D. Golberg, *J. Am. Chem. Soc.* **2003**, *125*, 2062.
- [4] a) R. Sen, A. Govindaraj, C. N. R. Rao, *Chem. Mater.* **1997**, *9*, 2078. b) P. M. Ajayan, C. Colliex, J. M. Lambert, P. Bernier, L. Barbedette, M. Tence, O. Stephan, *Phys. Rev. Lett.* **1994**, *72*, 1722. c) A. A. Setlur, J. M. Lauerhass, J. Y. Dai, R. P. H. Chang, *Appl. Phys. Lett.* **1996**, *69*, 345. d) V. Jourdain, H. Kanzow, M. Castignolles, A. Loiseau, P. Bernier, *Chem. Phys. Lett.* **2002**, *364*, 27. e) W. Q. Han, P. Redlich, F. Ernst, M. Rühle, *Appl. Phys. Lett.* **1999**, *75*, 1875. f) R. Ma, Y. Bando, T. Sato, *Adv. Mater.* **2002**, *14*, 366. g) P. M. Ajayan, T. W. Ebbesen, T. Ichihashi, S. Iijima, K. Tanigaki, H. Hiura, *Nature* **1993**, *362*, 522. h) W. Mickelson, S. Aloni, W. Han, J. Cumings, A. Zettl, *Science* **2003**, *300*, 467. i) W. Q. Han, C. W. Chang, A. Zettl, *Nano Lett.* **2004**, *4*, 1355. j) N. G. Chopra, R. J. Luyken, K. Cherrey, V. H. Crespi, M. L. Cohen, S. G. Louie, A. Zettl, *Science* **1995**, *269*, 966. k) Z. G. Chen, J. Zou, G. Q. Lu, G. Liu, F. Li, H. M. Cheng, *Appl. Phys. Lett.* **2007**, *90*, 103 117.
- [5] X. Blase, A. Rubio, S. G. Louie, M. L. Cohen, *Europhys. Lett.* **1994**, *28*, 335.
- [6] J. J. Pouch, A. Alterovitz, *Synthesis and Properties of Boron Nitride*, Trans Tech, Zurich **1990**.
- [7] Z. Zhou, J. Zhao, Z. Chen, X. Gao, J. P. Lu, P. V. R. Schleyer, C.-K. Yang, *J. Phys. Chem. B* **2006**, *110*, 2529.
- [8] Y. Chen, J. F. Gerald, J. S. Williams, S. Bulcock, *Chem. Phys. Lett.* **1999**, *299*, 260.
- [9] a) S. Y. Bae, H. W. Seo, J. Park, Y. S. Choi, J. C. Park, S. Y. Lee, *Chem. Phys. Lett.* **2003**, *374*, 534. b) C. C. Tang, M. L. De la Chapelle, P. Li, Y. M. Liu, H. Y. Dang, S. S. Fan, *Chem. Phys. Lett.* **2001**, *342*, 492. c) L. T. Chadderton, Y. Chen, *J. Cryst. Growth* **2002**, *240*, 164.
- [10] J. J. Velazquez-Salaz, E. Munoz-Sandoval, J. M. Romo-Herrera, F. Lupo, M. Rühle, H. Terrones, M. Terrones, *Chem. Phys. Lett.* **2005**, *416*, 342.
- [11] K. F. Huo, Z. Hu, J. J. Fu, H. Xu, X. Z. Wang, Y. N. Lu, *J. Phys. Chem. B* **2003**, *107*, 11 316.
- [12] a) Y. Fan, Y. S. Wang, J. S. Lou, S. F. Xu, L. G. Zhang, L. N. An, H. Heinrich, *J. Am. Ceram. Soc.* **2006**, *89*, 740. b) Y. Moriyoshi, Y. Shimizu, T. Watanabe, *Thin Solid Films* **2001**, *390*, 26. c) S. Trasobares, O. Stephan, C. Colliex, W. K. Hsu, H. W. Kroto, D. R. M. Walton, *J. Chem. Phys.* **2002**, *116*, 8966. d) R. Z. Ma, Y. Bando, T. Sato, *J. Electron Microscop.* **2002**, *51*, 259.
- [13] L. Reimer, *Mater. Trans. JIM* **1998**, *39*, 873.
- [14] A. H. Morrish, *The Physical Principles of Magnetism*, Robert E. Krieger Publishing Company, Malabar, FL **1965**, p. 1983.
- [15] T. Oku, I. Narita, H. Tokoro, *J. Phys. Chem. Solids* **2006**, *67*, 1152.
- [16] W. S. Seo, J. H. Lee, X. M. Sun, Y. Suzuki, D. Mann, Z. Liu, M. Tera-shima, X. P. Yang, M. V. McConnell, D. G. Nishimura, H. Dai, *Nat. Mater.* **2006**, *5*, 971.